Astron. Astrophys. 87, 330–338 (1980)

ASTRONOMY AND ASTROPHYSICS

Iron Line Emission from the Alfvén Shell in X-ray Binaries

M. M. Basko

Institute of Theoretical and Experimental Physics, B. Cheremushkinskaya 25, SU-117259 Moscow, USSR

Received January 2; revised August 10, 1979

Summary. The paper presents a model in which the iron line emission $\varepsilon = 6$–7 keV, discovered in spectra of some X-ray binaries, is interpreted as a reradiation of the X-ray continuum in the gaseous shell at the Alfvén surface. The solid angle Ω subtended by the shell, its radius r_A, the Thomson optical thickness τ_T and the electron density n_e are treated as free parameters. The temperature and the ionization equilibrium are determined by the interaction with the external X-ray flux. The allowed range of variation of the shell parameters is evaluated from the requirement that the values of the iron line equivalent width predicted by the model agree with the observed ones. The restrictions imposed by such an agreement on the Alfvén shell in Her X–1 are shown to be compatible with the limitations deduced from the soft X-ray data. The model predicts a considerable width of the iron line profile, $\Delta\varepsilon > 200$ eV. The problem of escape of the line photons from the shell in the course of multiple resonance scattering is discussed in detail. A number of observational consequences and tests are proposed for the model under discussion.

Key words: X-ray spectroscopy – X-ray binaries

1. Introduction

A unique property of the iron line $\varepsilon = 6$–7 keV discovered recently in the spectra of some X-ray binaries (Sanford et al., 1975; Serlemitsos et al., 1975; Pravdo et al., 1977; Becker et al., 1978b) is huge values of its equivalent width, $W \sim 0.3$–1 keV. Attempts to give a simple and straightforward interpretation to this powerful line emission encounter serious difficulties. First, this cannot be K_α fluorescence in the atmosphere of the optical counterpart of the X-ray source (Hatchett and Weaver, 1977; Basko, 1978a) because the latter

(1) has smaller equivalent widths, $W = \text{few} \times 10$ eV;

(2) shows a strong correlation with the orbital phase, which contradicts the observations of Her X–1 (Pravdo et al., 1977) and Cyg X–3 (Becker et al., 1978a);

(3) is centered at $\varepsilon = 6.40$ keV and has a small spectral width $\Delta\varepsilon \lesssim 30$ eV, which is in a disagreement with the measurements of Kestenbaum et al. (1977).

And even when one adds the fluorescence of an accretion disk and that of a stellar wind, the theoretical values of W for the HZ Her/Her X–1 system (Basko, 1978a) are still 3–5 times less than the observed ones.

Another possibility – formation of the line in the immediate vicinity of the X-ray photosphere – leads to even smaller values of the equivalent width. For accretion disks this was demonstrated by Mészàros (1974) who obtained $W < 10$ eV. Similar estimates can be also performed for the accretion to the surface of the neutron star. If one assumes that the accreting material falls onto $\sim 1/100$ (a typical value in the theory of X-ray pulsars) of the total surface area of Her X–1, then the photoionization rate of Fe^{+25} in its atmosphere is $\gamma^{+25} \approx 7.3\,10^{12} L_{37}\,s^{-1}$. From the shape of the Her X–1 spectrum one estimates an electron temperature $T \gtrsim 10^8$ K, which corresponds to the height scale $H \approx 10^2$ cm. The radiative recombination coefficient $\alpha_{\text{tot}}^{+25} \approx 1.3\,10^{-12}\,\text{cm}^3\,\text{s}^{-1}$, and the fraction of Fe^{+25} ions at the Thomson optical depth $\tau_T = 1$, where the electron density $n_e = (\sigma_T H)^{-1} \approx 1.5\,10^{22}\,\text{cm}^{-3}$, is $x^{+25} \approx 10^{-3}$. Under these conditions the principal mechanism of populating the $2p$ levels of Fe^{+25} is recombination, and from Eqs. (2) and (4a) of this paper [in Eq. (2) one must set $\Omega = 4\pi/100$, $r_A = R = 10^6$ cm, $\delta = 10^2$ cm] one gets $W \sim 1$ eV for a solar iron abundance. The line photons created at greater Thomson depths, $\tau_T > 1$, do not contribute to the observed feature because after two or three scatterings by electrons with temperature $T \gtrsim 10^8$ K they spread over a spectral interval $\Delta\varepsilon \sim \varepsilon$.

The right order of magnitude of the iron line equivalent width was obtained by Ross et al. (1978) in the model of a uniform gas sphere with Thomson optical radius $\tau_T = 6$, surrounding a point X-ray source in the center. This model, being undoubtedly closer to reality than that adopted by Felten et al. (1972), is however too strong an idealization to be applied to specific X-ray sources and to be compared with specific observational data. The other serious shortcoming of calculations by Ross et al. (1978) is that the density, temperature, and radius of the gaseous sphere have been fixed as if they were independent parameters, rather than to have been calculated in a self-consistent way.

This present paper is an attempt to explain the iron line observed in Her X–1 and other X-ray binaries as an emission from a plasma layer which is expected to form at the Alfvén surface, where the exterior accretion pattern is destroyed by a strong magnetic field of the neutron star (Lamb et al., 1973). Below, this plasma layer is called the Alfvén shell. The potential importance of the Alfvén shell for the models of binary X-ray pulsars has been realized when trying to interpret the observed pulse profile and soft X-ray emission in Her X–1 (McCray and Lamb, 1976; Basko and Sunyaev, 1976; Sunyaev, 1976a). Here it is shown that if one sets as a goal to explore the maximum possible iron line emission from the Alfvén shell, then it gets the values of W and other line characteristics that are in a reasonable agreement with the observations. The allowed range of the shell parameters variation

Table 1. The values of physical parameters in the Alfvén shell and the equivalent width of the iron line for a series of models with $L_{37}=5.8$, $r_8=1.3$, $\Omega=2\pi$, $\tau_T=1$, $Y_{\mathrm{Fe}}=1$

$n_e\,(10^{18}\,\mathrm{cm}^{-3})$	0.1	0.3	1.0	3.0	10
$\xi\,(\mathrm{erg\,cm\,s}^{-1})$	$3.43\,10^4$	$1.14\,10^4$	$3.43\,10^3$	$1.14\,10^3$	343
$T\,(10^6\,\mathrm{K})$	39.9	27.6	10.8	3.44	0.98
x^{+25}	0.0171	0.0657	0.310	0.400	0.0932
x^{+24}	$9.64\,10^{-5}$	$1.53\,10^{-3}$	0.052	0.479	0.903
y^{+7}	$5.23\,10^{-5}$	$2.07\,10^{-4}$	$1.62\,10^{-3}$	0.0146	0.121
W^{+25} (eV)	3.0	12	66	100	25
W^{+24} (eV)	0.047	0.77	29	290	590
$\tau_{ff}\,(\varepsilon=kT)$	$1.1\,10^{-8}$	$1.2\,10^{-7}$	$1.1\,10^{-5}$	$1.8\,10^{-3}$	0.49
$\tau\,(2^3P_1-1^1S_0)$	$6.21\,10^{-3}$	0.12	6.5	106	370
$\tau_{th}\,(2^3P_1-1^1S_0)$	$3.8\,10^5$	$3.8\,10^5$	$3.5\,10^5$	$2.6\,10^5$	$9.2\,10^4$

is shown to be compatible with the constraints (McCray and Lamb, 1976) imposed by the requirement that the same shell accounts for the soft X-ray emission in Her X–1. All numerical estimates are performed for the HZ Her/Her X–1 system, but most of the theoretical conclusions are quite general.

2. General Analysis of the Model

Since a complicated theoretical problem of the physical and geometrical structure of the Alfvén shell has not been solved yet, I shall treat it as an open uniform gaseous shell located at a radius r_A and subtending a solid angle Ω as seen from the neutron star, without any further specification of its geometry. Having fixed the cosmic chemical composition, I need to specify also the electron number density n_e and the Thomson optical thickness τ_T, in order to determine the physical conditions in the shell illuminated by the central X-ray source with the total luminosity L. The four quantities Ω, r_A, n_e, and τ_T will be treated as free parameters of the model, whose range of variation is to be determined from the comparison of theoretical values of the iron line equivalent width with the observed ones.

I assume further that the optical thickness of the Alfvén shell $\tau_T \lesssim 1$, and evaluate its temperature and ionization stage in the optically thin approximation, when they are completely determined (for a fixed spectrum of illuminating X-rays) by the value of parameter

$$\xi = L/n_e r_A^2 = 10^3\, L_{37}\, n_{18}^{-1}\, r_8^{-2}\,\mathrm{erg\,cm\,s}^{-1} \tag{1}$$

(Tarter et al., 1969; Buff and McCray, 1974). Here $L_{37}=L/10^{37}\,\mathrm{erg\,s}^{-1}$, $n_{18}=n_e/10^{18}\,\mathrm{cm}^{-3}$, $r_8=r_A/10^8$ cm. The condition $\tau_T \lesssim 1$, while greatly simplifying the calculations, does not seem to be particularly restrictive in our problem because, even when the actual optical thickness $\tau_T \gg 1$, the decrease of the X-ray intensity in the course of inward diffusion and the broadening of the line in the course of outward diffusion (see Sect. 4.3) result in that only a surface layer of the shell with $\tau_T \sim 1$, facing the neutron star, serves as an effective source of the line photons. Thus, to estimate within say a factor of ~ 3 the iron line intensity from an open shell of a large surface density $\tau_T \gg 1$, one can safely use the value $\tau_T = 1$.

In the analysis that follows I use a number of physical approximations whose validity can be verified only *a posteriori*, after plasma parameters in the shell have been determined. Thus an assumption that all the resonance photons created in the shell ultimately escape is extensively discussed in Sect. 4. Under this assumption the expression for the line equivalent width can be written as

$$W = \beta n_e n_{\mathrm{Fe}} \Omega r_A^2 \delta \varepsilon_l \varepsilon_{\max}/L = w(\xi)\tau_T \Omega Y_{\mathrm{Fe}}\,. \tag{2}$$

Here I have introduced the excitation coefficient β ($\mathrm{cm}^3\,\mathrm{s}^{-1}$) such that $\beta n_e n_{\mathrm{Fe}}$ is the number of excitations of iron ions to the level $n=2$ per $1\,\mathrm{cm}^3$ per 1 s; $\delta = \tau_T/\sigma_T n_e$ is the geometrical thickness of the shell, ε_l is the energy of the line photons. The spectrum of the X-ray star, that is used here and below, is given by Eq. (13) where $\varepsilon_{\max} = 30$ keV. The iron number density n_{Fe} is represented as

$$n_{\mathrm{Fe}} = 3\,10^{-5}\, n_{\mathrm{H}} Y_{\mathrm{Fe}}\,. \tag{3}$$

Having established the basic model parameters (see Table 1), one readily ascertains that the principal mechanism, responsible for the creation of $n=2$ excited states in iron ions, is recombination by which any electron that recombines to any excited level $n \geqq 2$ of Fe^{+25} and Fe^{+24} gives rise to a photon in one of the four basic lines comprising the observed feature $\varepsilon_l = 6.7$ keV (for details see Sects. 3.3 and 4.1)[1]. The relative contribution of the electron impact excitation never exceeds 1%. Under such conditions the excitation coefficient β, written separately for Fe^{+25} and Fe^{+24} ions, is

$$\beta^{+25} = (\alpha_{\mathrm{tot}}^{+25} - \alpha_1^{+25})(1 - x^{+25} - x^{+24}), \tag{4a}$$

$$\beta^{+24} = (\alpha_{\mathrm{tot}}^{+24} - \alpha_1^{+24})x^{+25}, \tag{4b}$$

where $\alpha_1^{+n}(\alpha_{\mathrm{tot}}^{+n})$ is the radiative recombination coefficient to the ground state (summed over all states) of Fe^{+n}; x^{+n} is the fraction of Fe^{+n} ions. Note that the approximation $x^{+26}+x^{+25}+x^{+24}=1$ used below to calculate the ionization equilibrium implies that W^{+24} represents in fact the sum of equivalent widths of $L \to K$ transitions in all ions Fe^{+n} with $n \leqq 24$ (see Sect. 3.4). Symbols W, w, and β, when used without superscripts, refer to the total iron line emission, with all components lumped together.

1 When combined with the fact that the iron is ionized exclusively by the X-ray continuum from the central source, this justifies the use of the term "fluorescence" for the line emission mechanism under discussion. The lower ions are excited directly by the K-shell photoionization

For fixed X-ray spectrum and chemical composition, the quantity

$$w(\xi)=1.21\,10^{16}\,\beta\xi^{-1}\,\mathrm{eV} \tag{5}$$

depends on parameter ξ only. Its behaviour, as calculated for $n_{Fe}=3\,10^{-5}\,n_H$, $n_O=4.4\,10^{-4}\,n_H$, is shown in Fig. 1. It can be easily investigated in two limiting cases:

(1) the iron is almost completely ionized, $x^{+24}\ll x^{+25}\ll 1$, which occurs at $\xi\gtrsim 10^4$ when $T\gtrsim 2\,10^7$ K;

(2) the iron is predominantly in the form of ions with the filled K-shell, $x^{+25}\ll 1$, $1-x^{+24}\ll 1$, – which occurs at $\xi\lesssim 300$ when $T\lesssim 10^6$ K.

In case (1) $\beta^{+25}\gg\beta^{+24}$, and

$$w\approx w^{+25}=1.21\,10^{16}[\alpha_{tot}^{+25}(\xi)-\alpha_1^{+25}(\xi)]\,\xi^{-1}\,\mathrm{eV}, \tag{6}$$

i.e. the iron line equivalent width rapidly increases with the decreasing ξ. In case (2) $\beta^{+24}\gg\beta^{+25}$ and the function $w(\xi)$ approaches its limiting value

$$w_{max}=130[1-\alpha_1^{+24}(\xi)/\alpha_{tot}^{+24}(\xi)]\,\mathrm{eV}\approx 107\,\mathrm{eV}, \tag{7}$$

that is obtained from Eqs. (5), (4b), and (14b). Apart from a weakly varying factor $(1-\alpha_1^{+24}/\alpha_{tot}^{+24})$, the limiting value w_{max} does not depend on the chemical composition and is determined exclusively by the shape $L^{-1}(dL/d\varepsilon)$ of the X-ray spectrum above the K-shell threshold ε_{th} – with which it scales as

$$w_{max}\propto\frac{1}{L}\int_{\varepsilon_{th}}^{\infty}\frac{dL}{d\varepsilon}\left(\frac{\varepsilon_{th}}{\varepsilon}\right)^{2.84}\frac{d\varepsilon}{\varepsilon}. \tag{8}$$

The limit (7) stems from the fact that any photon from the ionizing continuum absorbed in the shell can create at most one photon in the line.

Thus, we arrive at a conclusion that the equivalent width of the iron line emitted by the Alfvén shell is limited by the value

$$W_{max}=w_{max}\tau_T\Omega Y_{Fe}=107\,\tau_T\Omega Y_{Fe}\,\mathrm{eV}, \tag{9}$$

where the second equality sign applies to Her X–1. The values of W observed in Her X–1 range from ~ 200 eV to ~ 500 eV (Pravdo et al., 1977). Since one can hardly expect $\Omega>2\pi$ in Her X–1, the corollary of the above conclusion is that for the cosmic iron abundance $Y_{Fe}\approx 1.4$ *the observed values* $W\sim 500$ eV *can be explained if only* $\tau_T>0.5$ *and* $\xi<10^3$.

The optical thickness of the Alfvén shell $\tau_T>0.5$ can be understood in principle if the accreting material forms a disk beyond r_A, but it contradicts to a spherically-symmetric infall because in the latter case $\tau_T<0.1$ (Basko, 1977). If the plasma shell is to be supported by the dipole magnetic field of the neutron star, it must be close enough to the stellar surface, namely

$$r_A\lesssim 0.43\left(\frac{\mu^2\sigma_T}{GMm_p\tau_T}\right)^{1/4}=10^8\,\tau_T^{-1/4}\mu_{30}^{1/2}(M/M_\odot)^{-1/4}\,\mathrm{cm}, \tag{10}$$

where μ_{30} is the dipole magnetic moment of the neutron star in units of 10^{30} Gauss cm^3, and M is its mass. This value of r_A is a factor of 2–3 less than a simple pressure-balance estimate (Lamb et al., 1973)

$$r_A^{(0)}=2.9\,10^8\,\mu_{30}^{4/7}(L_{37}R_6)^{-2/7}(M/M_\odot)^{1/7}\,\mathrm{cm} \tag{11}$$

(here R_6 is the radius R of the neutron star in units of 10^6 cm), and seems to be in a reasonable agreement with other theoretical estimates of r_A based on dynamical models of the interface between the disk and the magnetosphere, although the latter are sometimes contradictory and range from $r_A<0.2\,r_A^{(0)}$ (Scharlemann, 1978) to $r_A\approx 0.7\,r_A^{(0)}$ (Gosh and Lamb, 1978).

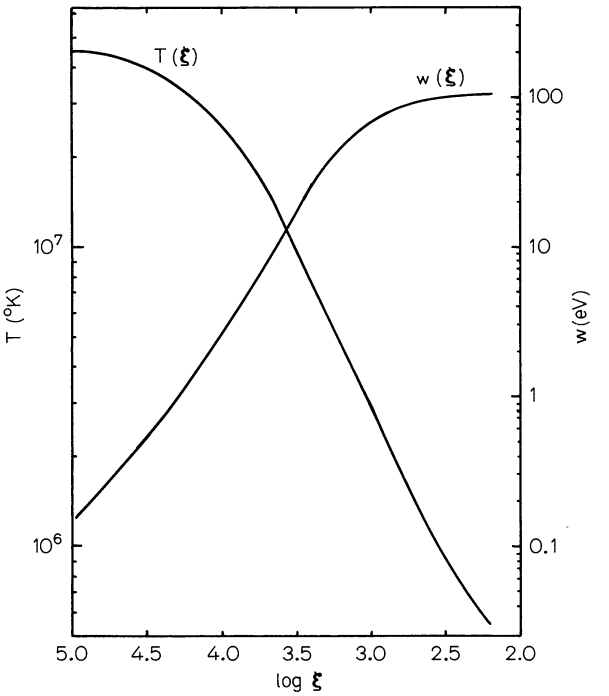

Fig. 1. The electron temperature T (left-hand ordinates) and the "reduced" iron line equivalent width w (right-hand ordinates) as functions of the parameter $\xi=L/n_e r_A^2$

One more necessary condition that should be satisfied in a self-consistent model of the Alfvén shell is

$$p+\varrho v^2\lesssim H^2/8\pi\approx\mu^2/8\pi r_A^6, \tag{12}$$

where p, ϱ, and v are the pressure, density and velocity of the shell plasma. The physical meaning of inequality (12) is that the magnetic stresses should be strong enough to force the accreting matter to leave the disk plane and spread over a large solid angle $\Omega>1$. Since the lower limit to v is rather uncertain, we can use only a weak version of (12), with $v=0$, to constrain the density variation in the shell when Ω, τ_T, and r_A are fixed.

As direct estimates show, all the above restrictions still leave a reasonably wide range in which the basic parameters of the shell can vary. For instance, any of the series of models proposed by McCray and Lamb (1976) to account for the soft X-ray emission from Her X–1 can be used to explain the observed fluxes in the iron line. As an illustrative example, I calculate the iron line emission from a set of model shells with the same values of all parameters as in model 2 of McCray and Lamb (1976), except for the electron density n_e which I vary in the interval $10^{17}\,\mathrm{cm}^{-3}\leqq n_e\leqq 10^{19}\,\mathrm{cm}^{-3}$. The fixed parameters are: $L_{37}=5.8$, $M=1.33\,M_\odot$, $R_6=1.5$, $\mu_{30}=2.1$, $\Omega=2\pi$, $\tau_T=1.1$, $r_8=1.3$. The results of calculations are presented in Table 1. The approximations and atomic physics used in these calculations are discussed below.

3. Thermal Balance and Atomic Processes

3.1. Thermal Balance

To evaluate the equilibrium temperature $T(\xi)$ for $\xi\gtrsim 300$, one has to include into the equation of thermal balance the following

processes (Buff and McCray, 1974): Compton scattering of the illuminating X-rays, bremsstrahlung cooling, heating and cooling by photoionization and recombination of iron and oxygen ions. General formulae for these cooling and heating mechanisms can be found in the above mentioned paper by Buff and McCray (1974). Since Compton heating is rather sensitive to a hard tail of the X-ray spectrum, I use one of the most detailed approximations to the observed spectrum of Her X–1 in 2–60 keV region (Becker et al., 1977; Pravdo et al., 1978):

$$\frac{\varepsilon_{\max}}{L}\frac{dL}{d\varepsilon}=\begin{cases}1, & \varepsilon\leqq 20\,\mathrm{keV},\\ \exp[(20\,\mathrm{keV}-\varepsilon)/10\,\mathrm{keV}], & \varepsilon>20\,\mathrm{keV},\end{cases} \tag{13}$$

where $\varepsilon_{\max}=30$ keV. The photoionization heating and the recombination cooling have been evaluated under the same approximations as the ionization equilibrium (see Sect. 3.2). Here it should be noted only that the optically thin approximation breaks down for the ionizing continuum of O^{+7} near the threshold $\varepsilon\sim\varepsilon_{th}$ when $\xi\lesssim 10^3$. But the attenuation of the ionizing continuum at $\varepsilon\sim\varepsilon_{th}$ does not necessarily result in a corresponding decrease of the heating rate. The heating rate is directly proportional to the mean energy $\langle\varepsilon\rangle$ of absorbed photons and to the number of photoionizations of O^{+7} per 1 s, which is equal to the number of recombinations onto O^{+8}. As compared to the optically thin case, the deficiency in photons with $\varepsilon\sim\varepsilon_{th}$ will result in a decrease of the fraction y^{+8} of completely stripped oxygen but, if say y^{+8} is still $\gtrsim 0.5$ due to the unattenuated continuum at $\varepsilon\sim(2\text{–}3)\varepsilon_{th}$, the number of recombinations onto O^{+8} may decrease only slightly, while the mean energy $\langle\varepsilon\rangle$ will increase. For this reason, complicated optically thick calculations do not seem to be warranted, and the optically thin formulae are used throughout.

The cooling in the resonance line of He^+, that might become important at $\xi\sim 300$ (Buff and McCray, 1974) can be safely neglected here because these values of ξ are attained at such a high density in the shell that the electron de-excitation of $2p$-levels of He^+ dominates over their radiative decay, while the optical depth in the line $\gtrsim 10^3$. Under such conditions only a small fraction of L_α photons of He^+ created in the shell escape. The cooling rate in the resonance line of O^{+7} never exceeds few per cent of the bremsstrahlung cooling rate.

If the Alfvén shell is dense enough, it becomes opaque for the bremsstrahlung photons and its cooling occurs from the surface. This happens when $\tau_{ff}(\varepsilon=kT)\approx 2$. In the present calculations I made no account of this effect because it does not influence the iron line equivalent width, and only the values of $\tau_{ff}(\varepsilon=kT)$ are given in Table 1. Note that once the shell becomes opaque for the free-free emission, its temperature stabilizes at some value and does not change in the course of further increase of its density, if all other shell parameters are fixed.

The function $T(\xi)$, calculated as outlined above for the iron and oxygen abundances $n_{\mathrm{Fe}}=3\,10^{-5}n_{\mathrm{H}}$, $n_{\mathrm{O}}=4.4\,10^{-4}n_{\mathrm{H}}$, is plotted in Fig. 1. The curve in Fig. 1 passes well above the analogous curve from Buff and McCray (1974) because the latter authors (i) took softer X-ray spectrum, and (ii) did not include the heating by photoionization of iron whose contribution amounts to $\sim 35\%$ at small ξ.

3.2. Ionization Equilibrium

Only three stages of iron ionization, $Fe^{+26,+25,+24}$, and two stages of oxygen ionization, $O^{+8,+7}$, have been included in calculations, and the ionization equilibrium has been determined from the following equations

$$\gamma^{+25}x^{+25}=\alpha_{\mathrm{tot}}^{+25}n_e(1-x^{+25}-x^{+24}), \tag{14a}$$

$$\gamma^{+24}x^{+24}=\alpha_{\mathrm{tot}}^{+24}n_e x^{+25}, \tag{14b}$$

$$(\gamma^{+7}+c^{+7}n_e)y^{+7}=\alpha_{\mathrm{tot}}^{+7}n_e(1-y^{+7}), \tag{15}$$

where y^{+7} is the fraction of O^{+7} ions. The effect of lower iron ions, $Fe^{+23}, Fe^{+22}, \ldots$, is discussed in Sect. 3.4. Helium and hydrogen are assumed to be fully ionized.

To calculate the photoionization rates γ^{+n} for hydrogenlike ions, the expression

$$\sigma_{ph}(\varepsilon)=\frac{6.3\,10^{-18}}{Z^2}\left(\frac{\varepsilon_{th}}{\varepsilon}\right)^{2.84}\mathrm{cm}^2, \tag{16}$$

approximating within the error $\sim 10\%$ in the interval $1\leqq\varepsilon/\varepsilon_{th}\lesssim 6$ the results of Burgess (1964), was used. When evaluating γ^{+24}, the nuclear charge Z in Eq. (16) was set equal to 25.7 (Bethe and Salpeter, 1957) and the numerical coefficient was doubled. The collisional ionization coefficient for O^{+7} was estimated according to the formula

$$c^{+7}=1.1\,10^{-10}\frac{\chi^{1/2}}{0.4+\chi}e^{-\chi}\,\mathrm{cm}^3\,\mathrm{s}^{-1},\quad \chi=\frac{1.01\,10^7\,\mathrm{K}}{T}, \tag{17}$$

approximating the calculations by Lotz (1967) to an accuracy $\sim 10\%$. The rates of collisional ionization of the iron ions are negligible as compared to their photoionization rates.

The radiative recombination coefficients $\alpha_{\mathrm{tot}}^{+n}$ summed over all excited states (as well as those to the ground state, α_1^{+n}) were taken from Burbidge and Gould (1963). Dielectronic recombination onto Fe^{+25} was neglected since its contribution does not exceed 25% at $T=5\,10^7$ K and drops rapidly with a decreasing temperature. The triple recombination onto iron and oxygen ions can also be neglected at densities $n_e<10^{21}\,\mathrm{cm}^{-3}$.

3.3. Atomic Transitions in Iron Ions

The four basic transitions that contribute in our case to the iron line emission are: two allowed $2p_{1/2,3/2}\to 1s_{1/2}$ ($\varepsilon_l=6950$ eV, 6970 eV) transitions in Fe^{+25} ions with the radiative decay rate $A=2.9\,10^{14}\,\mathrm{s}^{-1}$, and allowed $2^1P_1\to 1^1S_0$ ($\varepsilon_l=6701$ eV) and intercombination $2^3P_1\to 1^1S_0$ ($\varepsilon_l=6668$ eV) transitions in Fe^{+24} ions with $A=4.73\,10^{14}\,\mathrm{s}^{-1}$ and $A=4.32\,10^{13}\,\mathrm{s}^{-1}$ (Vainshtein and Safronova, 1977). At high densities, that one needs for a condition $\xi<10^3$ to be satisfied, all other ways of the radiative decay of $n=2$ states in Fe^{+25} and Fe^{+24} ions are quenched by collisions with charged particles. Evaluating the rates of collisional $2S\to 2P$ transitions from the hydrogenlike formulae derived by Jacobs (1972), who took into account collisions with electrons and protons, we find that for the $2s_{1/2}$ state of Fe^{+25} the collisional and radiative decay rates become equal at $n_e\approx 1.3\,10^{17}\,\mathrm{cm}^{-3}$, while the collisional transitions $2^1S_0\to 2^1P_1$ and $2^3S_1\to 2^3P_{0,1,2}$ quench the radiative decays of $2S$ states of Fe^{+24} when $n_e\gtrsim 1.8\,10^{18}\,\mathrm{cm}^{-3}$ and $n_e\gtrsim 1.7\,10^{17}\,\mathrm{cm}^{-3}$ respectively. If, however, the electron density $n_e<10^{19}\,\mathrm{cm}^{-3}$, an appreciable emission may arise also from the $2^3P_2\to 1^1S_0$ transition ($\varepsilon_l=6683$ eV, $A=7.83\,10^9\,\mathrm{s}^{-1}$). Transitions between the singlet and triplet groups of states can be neglected.

Below it is shown that the four lines associated with the four main transitions are rather narrow and quite distinct from each other locally, at each point of the Alfvén shell, – which is important for the escape probabilities – but they merge into two

(or even one) broad features for a distant observer. For this reason only combined line intensities for each of the two ions, Fe^{+25} and Fe^{+24}, are given everywhere.

3.4. The Effect of Lower Stages of Iron Ionization

The most crude approximation in the above discussion was to ignore the lower stages of iron ionization – Fe^{+23}, Fe^{+22}, ... As direct estimates show, these ions start to dominate at $\xi \lesssim 500$. The most serious must be the revision of Fe^{+25} fractions – for $\xi \lesssim 500$ the values of x^{+25} in Table 1 should be decreased by more than a factor of 2. As a consequence, the equivalent widths W^{+25} must be reduced by the same factor, because for fixed n_e and T^2 they are proportional to the number of Fe^{+25} ionizations. It should be noted however, that in this range of ξ values $W^{+25} \lesssim 0.1\, W^{+24}$, and the lines of Fe^{+25} are practically unobservable.

In contrast to W^{+25}, the analogous decrease of x^{+24} in favour of x^{+23}, x^{+22}, ... does not lead to a noticeable change of W^{+24}, if the latter quantity is understood as a sum of equivalent widths of Fe^{+24}, Fe^{+23}, Fe^{+22}, ... K-lines, because the total number of K-ionizations in all these ions remains almost constant. The probability to emit a K-photon after the ionization of Fe^{+24} is $\omega_K \approx 5/6$ (the fraction of recombinations to the ground state of Fe^{+24} at $T \sim 10^6$ K is $\approx 1/6$); the fluorescence yields of Fe^{+23} and of $Fe^{+22}-Fe^{+0}$ ions are respectively $\omega_K = 1$ and $\omega_K \approx 0.6$–0.34. Thus, the presence of Fe^{+23} ions at the expense of Fe^{+24} effectively increases W^{+24}, while the presence of Fe^{+22} decreases W^{+24}, and these two effects to a large extent compensate each other. As a result, the uncertainty in W^{+24} values presented in Table 1 and given by Eq. (7) scarcely exceeds 10%–20%.

The K-ionization of Fe^{+22} is followed by the emission of a satellite of some heliumlike transition, but because of the large spectral width of the observed line (see Sect. 4.3) this fact has no observational consequenses.

4. Diffusion of Line Photons

In this section I verify the above approximation that all the line photons finally escape from the Alfvén shell. This has to be done only for those lines that undergo resonance scattering, namely for two lines of $Fe^{+25}(2p_{1/2,\,3/2} \to 1s_{1/2})$ and for two lines of $Fe^{+24}(2^{1,3}P_1 \to 1^1S_0)$. To this end, I first calculate the upper limits to the optical thickness of the shell in these transitions, and then demonstrate that they never exceed the corresponding values of the thermalization length τ_{th} – a mean optical distance by which a line photon displaces in the course of resonance scattering from its "birth place" before it undergoes a "true" absorption or, in other words, perishes.

4.1. Line Opacities

To estimate the optical thickness in a line, it is first necessary to establish the dominant mechanism of its profile broadening. Relatively simple semi-classical estimates (Basko, 1978b) show that pressure effects can be neglected for the iron lines as compared to the radiative damping so long as $n_e < 10^{21-22}\,\mathrm{cm}^{-3}$. The natural widths $\Delta\varepsilon_\gamma$ of $2p_{1/2,3/2} \to 1s_{1/2}$ lines of Fe^{+25}, and of $2^1P_1 \to 1^1S_0$ and $2^3P_1 \to 1^1S_0$ lines of Fe^{+24} are respectively 0.19 eV, 0.31 eV, and 0.028 eV; their Doppler width is

$$\Delta\varepsilon_D = \varepsilon_l (2kT/Am_pc^2)^{1/2} = 0.4\, T_6^{1/2}\,\mathrm{eV}, \tag{18}$$

where $T_6 = T/10^6$ K.

In principle, one could expect much more significant broadening from the macroscopic motions. But if the plasma in the shell is threaded by magnetic field lines – which seems to be the most likely possibility – then the maximum gradient of the macroscopic velocity v that one can adopt *a priori* is of the order of gravitational potential gradient,

$$\frac{dv}{v} \approx -\tfrac{1}{2}\frac{dr}{r}. \tag{19}$$

Taking into account that in all cases of practical interest the thickness of the shell $\delta \ll r_A$, we get

$$\Delta\varepsilon_m = \varepsilon_l \frac{\Delta v}{c} \lesssim \varepsilon_l \frac{\delta}{2r_A}\frac{0.3v_{ff}}{c} = 0.82\tau_T r_8^{-3/2} n_{18}^{-1} (M/M_\odot)^{1/2}\,\mathrm{eV}, \tag{20}$$

which is less than $\Delta\varepsilon_D$ in the most interesting cases when $W \gtrsim 300$ eV (see Table 1). In deriving Eq. (20) I made use of the condition $v \lesssim 0.3\, v_{ff}$ (v_{ff} is the local free-fall velocity) which is suggested by the earlier calculations (Basko, 1977) of the plasma flow in the Alfvén shell.

The above estimates convince us that the scattering cross-section σ_s in the line center must be evaluated with the Doppler width (18), namely

$$\sigma_s = \pi^{-1/2}\frac{2\pi\hbar}{\Delta\varepsilon_D}\frac{\pi e^2}{m_e c} f_{12} = \frac{1}{4\pi^{1/2}}\frac{g_2}{g_1}\frac{\Delta\varepsilon_\gamma}{\Delta\varepsilon_D}\lambda_{12}^2, \tag{21}$$

where g_2 and g_1 are the statistical weights of the upper and lower levels, λ_{12} is the wavelength of the transition, and f_{12} is its oscillator strength. On the other hand, the Doppler width (18) is certainly a lower bound to the actual width of the line contour. Thus, the optical thickness of the Alfvén shell in the four basic iron lines cannot exceed the values

$$\begin{aligned}
\tau(1s_{1/2} - 2p_{1/2}) &= 800\, x^{+25} T_6^{-1/2} \tau_T Y_{Fe},\\
\tau(1s_{1/2} - 2p_{3/2}) &= 1600\, x^{+25} T_6^{-1/2} \tau_T Y_{Fe},\\
\tau(1^1S_0 - 2^1P_1) &= 4400\, x^{+24} T_6^{-1/2} \tau_T Y_{Fe},\\
\tau(1^1S_0 - 2^3P_1) &= 410\, x^{+24} T_6^{-1/2} \tau_T Y_{Fe}.
\end{aligned} \tag{22}$$

The values of $\tau(1^1S_0 - 2^3P_1)$ calculated according to Eq. (22) are listed in Table 1.

From Eq. (21) one ascertains also that, as a rule, the shell is optically thick for transitions $(n \geqq 3) \to (n = 1)$ as well; for example

$$\tau(1s_{1/2} - 4p_{3/2}) = 110\, x^{+25} T_6^{-1/2} \tau_T Y_{Fe}. \tag{23}$$

The latter fact justifies the above conjecture that any act of recombination to the excited levels of Fe^{+25} and Fe^{+24} results ultimately in one of $(n=2) \to (n=1)$ transitions.

4.2. The Problem of Photon Escape from the Shell

In our case, the most efficient mechanisms of "true" absorption are the electron impact de-excitation and the photoionization from the excited level $n=2$. In the simplest case of a two-level

2 The inclusion of lower iron ions will have only a small effect on thermal equilibrium

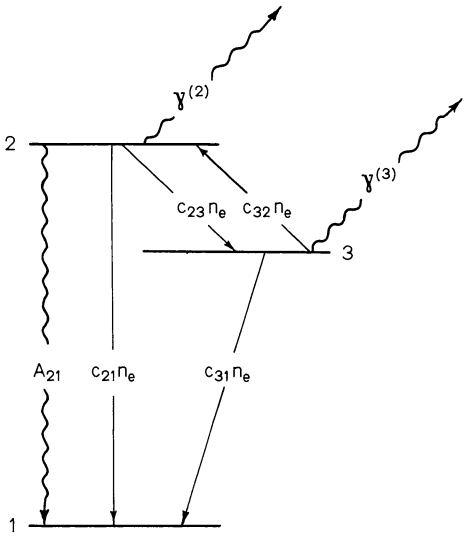

Fig. 2. The decay channels of an excited level 2 in a three-level system; ——— – collisional transitions, ~~~~~ – radiative transitions

system the probability for a line photon to perish in a single act of resonance scattering is

$$p_a = \frac{c_{21}n_e + \gamma^{(2)}}{A_{21} + c_{21}n_e + \gamma^{(2)}}, \tag{24}$$

where A_{21} is the radiative decay rate of the excited level 2, c_{21} is the electron impact de-excitation coefficient, and $\gamma^{(2)}$ is the photoionization rate for level 2. In our scheme level 2 designates one of the levels $2p_{1/2}$, $2p_{3/2}$ in Fe^{+25}, or 2^1P_1, 2^3P_1 in Fe^{+24}. On average, every line photon gets absorbed after p_a^{-1} individual acts of resonance scattering and, in order to evaluate τ_{th}, one has to calculate the mean optical distance by which a photon displaces to this moment.

The situation becomes more complicated when beside level 2 there is a level 3 such that the transition $1\to3$ is forbidden, while the transitions $2\to3$ and $1\to2$ are allowed (the level $2s_{1/2}$ in Fe^{+25}, or the levels 2^1S_0 and 2^3S_1 in Fe^{+24}). In this case collisional transitions $2\to3$ effectively prolong the lifetime of the excited state, and there appears a finite probability of a non-coherent (in the rest frame of the ion) scattering. Indeed, in the two-level case it was tacitly assumed that the line photons either perish ($c_{21}n_e$ and $\gamma^{(2)}$ branches) or undergo a coherent scattering (A_{21} branch), with a frequency in the rest frame of a scatterer remaining unchanged. With three levels, an additional channel $c_{23}n_e\to c_{32}n_e\to A_{21}$ (see Fig. 2) of scattering appears which, within the resonance, destroys any correlation between the photon frequencies before and after scattering. The probability of a "true" absorption in this case is

$$p_a = \left\{1 + A_{21}\Big/\left[\gamma^{(2)} + c_{21}n_e + c_{23}n_e\frac{\gamma^{(3)} + c_{31}n_e}{\gamma^{(3)} + c_{31}n_e + c_{32}n_e}\right]\right\}^{-1}$$
$$\approx \left[\gamma^{(2)} + c_{21}n_e + \frac{c_{23}}{c_{32}}(\gamma^{(3)} + c_{31}n_e)\right]\Big/A_{21} \ll 1, \tag{25}$$

while the probability of a non-coherent scattering is given by

$$p_{nc} = \frac{c_{23}n_e c_{32}n_e(1-p_a)}{(c_{32}n_e + \gamma^{(3)} + c_{31}n_e)(A_{21} + c_{21}n_e + c_{23}n_e + \gamma^{(2)})}$$
$$\approx c_{23}n_e/A_{21} \gg p_a. \tag{26}$$

In Eqs. (25) and (26) the conditions $A_{21} \gg c_{23}n_e \gg \gamma^{(2)} \approx \gamma^{(3)}$ and $c_{23} \gg c_{21}$ were used. It should be noted here that $c_{23}n_e$ is the rate of transitions resulting not from electron collisions only, but from collisions with other charged particles too. The formulae obtained by Jacobs (1972) were used to evaluate this quantity.

Thus, in a three-level case the $1\to2$ line photons get absorbed after p_a^{-1} scatterings on average, while every $p_{nc}^{-1}(\ll p_a^{-1})$ coherent scatterings are followed by a non-coherent one. Non-coherent resonance scattering is adequately described by a hypothesis of a complete frequency redistribution, but this hypothesis must be abandoned when discussing a coherent scattering of Fe^{+25} and Fe^{+24} resonance lines in a medium with electron density $n_e < 10^{21}\,cm^{-3}$ (Basko, 1978b). There would have been no need though to make any difference between the coherent and non-coherent cases, if the line photons perished within the Doppler core of the Voigt profile (Basko, 1978c), but this is not the case here. Ignoring the non-coherent scattering and estimating τ_{th} from Eq. (47b) of (Basko, 1978c), we obtain a lower bound to the thermalization length,

$$\tau_{th} > p_a^{-1} > \frac{A_{21}}{c_{21}n_e + \gamma^{(2)}}\left[1 + \frac{g_3}{g_2}\exp(\varepsilon_{32}/kT)\right]^{-1}, \tag{27}$$

because after any N successive acts of non-coherent scattering in the Lorentz wings the typical photon covers an optical distance $\langle\tau\rangle \approx (\Delta\varepsilon_\gamma/\Delta\varepsilon_D)N^2$ (Ivanov, 1969), while in the coherent case this distance is much smaller, $\langle\tau\rangle \approx N$ (Basko, 1978c). Here g_2 and g_3 are statistical weights of levels 2 and 3, $\varepsilon_{32} = E_2 - E_3$ is the energy of $2\to3$ transition. To derive Eq. (27), I made use of the equation of detailed balance connecting c_{32} with c_{23}, and of the condition $c_{31} < c_{21}$ valid for a forbidden transition $1\to3$, as well as assumed $\gamma^{(2)} = \gamma^{(3)}$, which is a resonable approximation for hydrogenlike ions (Burgess, 1964).

Numerical estimates according to Eq. (27) immediately demonstrate that the values of τ_{th} for every of the four main transitions in Fe^{+25} and Fe^{+24} always exceed by 1–2 orders of magnitude the optical thicknesses (22) of the Alfvén shell in corresponding lines. As an example, the lower limits to τ_{th} for the strongest transition $1^1S_0 - 2^3P_1$ are listed in Table 1. Thus, recalling that the Doppler broadening (18) is in fact the lower limit to the line widths, I conclude that *practically all iron line photons created in the Alfvén shell escape.*

4.3. Compton Scattering and the Observed Line Width

Since the Thomson optical thickness of the shell $\tau_T \sim 0.5$–1, while the optical depth with respect to the resonance scattering greatly exceeds 1, the typical line photon experiences at least one scattering by electron. After the very first such scattering a photon with the energy $\varepsilon_l = 6.7\,keV$ spreads due to the Doppler effect over the energy interval

$$\Delta\varepsilon = \varepsilon_l(4kT/m_ec^2)^{1/2} \approx 180\,T_6^{1/2}\,eV \tag{28}$$

(Chandrasekhar, 1960) and comes out of resonance. The Compton recoil has the same order of magnitude,

$$\Delta\varepsilon \approx -\varepsilon_l^2/m_ec^2 \approx -90\,eV. \tag{29}$$

The flow of gas along the Alfvén surface broadens the observed line profile by

$$\Delta\varepsilon \lesssim \varepsilon_l\frac{0.3v_{ff}}{c} \approx 110 r_8^{-1/2}(M/M_\odot)^{1/2}\,eV. \tag{30}$$

Thus, *the model being discussed predicts the width of the observed iron line profile to be* $\gtrsim$*200–300* eV.

At such width different transitions in one and the same ion blend, and one might hope to resolve the observed iron line in no more than two components corresponding to ions Fe^{+25} and Fe^{+24}. Note that the neglect of Compton scattering in the previous section is justified by the fact that its effect would be only to increase the escape probability.

5. Discussion

5.1. Soft X-ray Emission

The plasma in the Alfvén shell has been already proposed (McCray and Lamb, 1976; Basko and Sunyaev, 1976; Sunyaev, 1976a) as the most likely candidate for a source of soft, $\varepsilon = 0.1$–0.5 keV, X-ray emission discovered in Her X-1 by Shulman et al. (1975). The restrictions imposed on the shell parameters by such an interpretation agree very well with those derived from the requirement that the same shell accounts for the observed iron line emission. If one demands that the equivalent width $W \gtrsim 300$–500 eV, then one obtains a necessary condition $\tau_T \Omega Y_{Fe} > 3$–5, which is satisfied for the whole range of the shell parameters discussed by McCray and Lamb (1976). At the next step, having adopted $\tau_T = 1$, $\Omega = 2\pi$, $Y_{Fe} = 1 (n_{Fe} = 3\,10^{-5} n_H)$, one arrives at a condition $\xi \lesssim 10^3$, that is again compatible with all the models of McCray and Lamb (1976).

Note that the latter condition $\xi \lesssim 10^3$ provides a rather sensitive lower limit to the electron density in the shell, $n_e > 3\,10^{18}\,\mathrm{cm}^{-3}$, which in turn implies $T < 3\,10^6$ K. It is much more difficult to obtain a reliable upper bound for n_e, which, in our model, may be connected only with the line center shift from $\varepsilon_l = 6.70$ keV to $\varepsilon_l = 6.40$ keV as the lower stages of iron ionization start dominating. Thus, the observations of the soft X-rays and of the line emission may in some respect complement each other – while the former give a rather sensitive limit to the radial size r_A of the shell, the latter enables one to constraint its chemical composition (iron abundance) and the electron density n_e.

If the Alfvén shell in Her X-1 corotating with the neutron star is responsible both for the soft X-rays and for the iron line emission, the following observational test can be proposed: the 1.24 pulsations in soft X-rays $\varepsilon = 0.1$–0.5 keV must correlate in phase with the pulsations of the *absolute energy flux* in line – the maximum of the soft X-ray flux should always correspond to the maximum flux in line.

5.2. Recombination Continuum and K-Jumps

A salient feature of the line emission mechanism under discussion is that the line photons are created at the expense of photons from the ionizing continuum. To a corresponding suppression of the primary continuum one must add an emission resulting from direct recombinations to the ground state. Figure 3 illustrates the shape of the X-ray spectrum in 6–10 keV region averaged over all sight directions that one might expect from Her X-1 when $W \approx 400$ eV. This spectrum is highly idealized and should not be taken literally, but it demonstrates that the diminution of the continuum level at $\varepsilon \gtrsim 9$ keV is rather small, $\sim 15\%$, and needs a large counting statistics to be discovered. In reality, the recombination features of Fe^{+24} at $\varepsilon = 8.83$ keV and of Fe^{+25} at $\varepsilon = 9.28$ keV will be much less conspicuous than in Fig. 3 because of a number of smearing effects (see Sect. 4.3). If the screening by

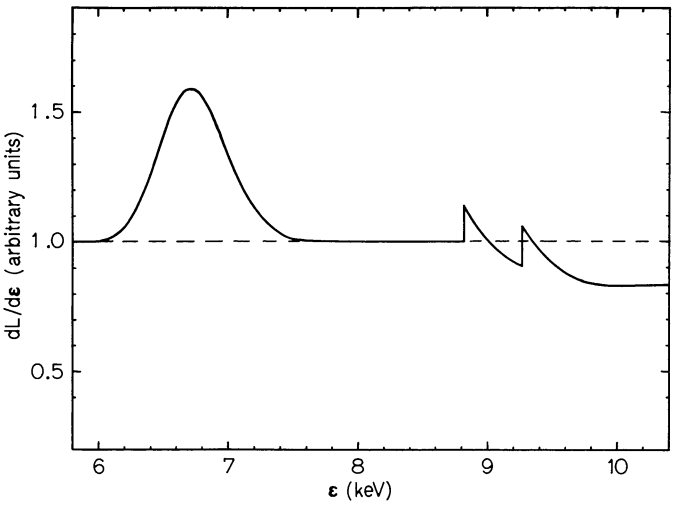

Fig. 3. An approximate shape of the X-ray spectrum in the vicinity of the iron line that one would expect from Her X-1 for $W \approx 400$ eV ($n_e = 3\,10^{18}\,\mathrm{cm}^{-3}$). The spectrum is averaged over the period of 1.24 pulsations

the Alfvén shell accounts for the pulsing behaviour of Her X-1 (McCray and Lamb, 1976; Basko and Sunyaev, 1976), then one should expect the deepest K-absorption between the pulses, where it can amount to $\sim 30\%$–40%.

Much more pronounced should be the absorption above the K-edge of O^{+7} ($\varepsilon_{th} = 870$ eV). If one requires $W > 300$ eV, then the optical thickness of the Alfvén shell just above the ionization threshold of O^{+7} is $\tau^{+7} \gtrsim 0.5$. The detection of this K-jump together with the oxygen line would be a strong evidence in favour of the model being discussed.

5.3. An Oxygen Line

If the ratio of oxygen to iron abundances n_O/n_{Fe} is not anomalously small, then the same mechanism that accounts for the iron line emission must excite the resonance line $\varepsilon_l = 653$ eV of a hydrogenlike oxygen ion O^{+7}. The calculations of its equivalent width W^{+7} are complicated, however, by a large optical depth in the ionizing continuum at $\xi < 10^3$, as well as by small values of the thermalization length τ_{th} as compared to the optical thickness in the line center.[3] The order-of-magnitude estimates show that, as the density in the shell increases, the equivalent width W^{+7} reaches its maximum value $W^{+7}_{max} \approx 30$–50 eV at $n_e \sim 3\,10^{18}\,\mathrm{cm}^{-3}$. The drop of the oxygen line intensity at high densities is due to a rapid rise of the de-excitation rate. Note that when estimating the excitation coefficient β^{+7}, one has to include also the electron impact excitation.

5.4. Iron Line Emission in Other X-ray Binaries

If one assumes that the model under consideration is general enough and can be applied to the class of X-ray binaries as a whole, then immediately the conclusion can be drawn that strong iron lines are to be found in the spectra of pulsating sources only,

3 It is not clear whether a hypothesis of complete frequency redistribution by resonance scattering is applicable to the oxygen line at densities $n_e \sim 10^{18-20}\,\mathrm{cm}^{-3}$

since it is X-ray pulsars that possess strong magnetic fields necessary to the formation of the Alfvén shell. To this one must add an empirical fact that the pulsating sources usually have harder X-ray continua, which is not the least important for high values of the equivalent width [cf. Eq. (8)]. And though the observational data, published up to now, are rather scarce, the above conclusion seems to agree with them. Among the best studied X-ray binaries strong iron lines have been detected in the spectra of Her X-1 (Pravdo et al., 1977), Cen X-3 (Swank, 1977), and 4U 0900–40 (Becker et al., 1978b) – well known X-ray pulsars, while all the efforts to find this line in the spectra of much brighter sources Sco X-1 and Cyg X-1 (Boldt, 1977), which do not pulsate, have been unsuccessful.

A special attention should be paid to the X-ray source Cyg X-3 which reveals the most powerful of all X-ray binary iron line emissions with $W\sim 1$–2 keV (Serlemitsos et al., 1975; Becker et al., 1978a). This source has not yet been proved to be an X-ray pulsar of the same type as Her X-1 and Cen X-3. Only one period, $p=4^h.8$, has been firmly established in its flux variations, which may conceivably represent the orbital motion as well as the spinning of the neutron star (Sunyaev, 1976b). Here I argue that the model above can be applied to this X-ray source too, not leading to any obvious contradiction with the observations.

First, the large values of the equivalent width $W\sim 1$ keV can be explained either by somewhat higher iron abundance, $n_{\rm Fe}\approx(6\text{–}8)\,10^{-5}n_{\rm H}$, or by the values of $\tau_T\sim 2$–3 for which the uncertainty in my estimates of W may be of the factor of ~ 2. Second, the fact that the absolute energy flux in the line remains almost constant (Pravdo, 1978) while Cyg X-3 undergoes transitions between low and high states, with the flux at $\varepsilon\sim 4$ keV changing by an order of magnitude (Serlemitsos et al., 1975), provides a strong evidence for the fluorescence to be the line emission mechanism, because the flux at $\varepsilon>8.8$ keV, responsible for the line excitation, does not show any noticeable change in such transitions (Serlemitsos et al., 1975).

The absence of variations in W with $4^h.8$ phase (Becker et al., 1978a) may be considered as an evidence for $4^h.8$ being an orbital period rather than that of a neutron star spin, because one would expect the flux in the line from a corotating Alfvén shell to anticorrelate with the primary X-ray flux from the neutron star surface, i.e. appreciable variations in W with the pulse phase, as is the case for example in Her X-1 (Pravdo et al., 1977).

The large values of W in Cyg X-3 could also be explained in principle as a fluorescence of the cocoon in a model proposed by Milgrom (1976). But the fluorescing shell in this model is located at $r\sim 10^{12}$ cm, which infers rather low values of parameter

$$\xi=\frac{L}{n_e r^2}\approx\frac{6\,10^{37}}{10^{13}(10^{12})^2}=6$$

and temperature $T\approx(2\text{–}4)\,10^5$ K. Under such conditions the iron is only weakly ionized, and the fluorescence occurs essentially at $\varepsilon_l=6.40$ keV. The measurements by Kestenbaum et al. (1977), that give $\varepsilon_l=6.84\pm0.17$ keV, favour the Alfvén shell model, though the later data from the same group (Kestenbaum et al., 1978), $\varepsilon_l=6.52\pm0.08$ keV, are compatible within 2σ limit with both interpretations.

6. Main Conclusions

From the above analysis I conclude that the powerful iron lines discovered in the spectra of several X-ray binaries can be – at least in principle – interpreted as a fluorescence of gas with cosmic heavy element abundancies in the Alfvén shell. The restrictions imposed by such an interpretation on the shell parameters in Her X-1 are in good agreement with the limitations derived from entirely different physical arguments, e.g. from the requirement that the same shell accounts for the observed characteristics of the soft X-rays. When applied to other less explored X-ray binaries, this interpretation does not lead to any serious contradiction with the existing observational data.

The model predicts that the iron line must appear to have a considerable spectral width, $\varepsilon/\Delta\varepsilon<30$, and be centered somewhere between $\varepsilon_l=6.70$ keV ($2^3P_1\to1^1S_0$ transition in Fe^{+24}) and $\varepsilon_l=6.40$ keV (K_α transitions in low ionized iron $Fe^{+0}-Fe^{+16}$), depending on the density in the shell. In this respect it is clearly distinct from the K_α fluorescence in the atmospheres of the normal companion and of the accretion disk, and in the stellar wind, which gives $\varepsilon/\Delta\varepsilon>200$. The latter result implies that the line profile could be scanned over with the aid of a detector of moderate spectral resolution, $\varepsilon/\Delta\varepsilon\sim 100$–$200$.

Acknowledgements. I wish to thank, L. A. Vainshtein for useful information on some atomic data, and the referee for a valuable criticism.

References

Basko, M.M.: 1977, *Astron. Zh. (Soviet Astron.)* **54**, 1051
Basko, M.M.: 1978a, *Astrophys. J.* **223**, 268
Basko, M.M.: 1978b, Preprint of the Space Research Institute No. 410, Academy of Sciences of the USSR
Basko, M.M.: 1978c, *Zh. Eksp. Teor. Fiz.* **75**, 1278
Basko, M.M., Sunyaev, R.A.: 1976, *Astron. Zh. (Soviet Astron.)* **53**, 950
Becker, R.H., Boldt, E.A., Holt, S.S., Pravdo, S.H., Rothschild, R.E., Serlemitsos, P.J., Smith, B.W., Swank, J.H.: 1977, *Astrophys. J.* **214**, 879
Becker, R.H., Robinson-Saba, J.L., Boldt, E.A., Holt, S.S., Pravdo, S.H., Serlemitsos, P.J., Swank, J.H.: 1978a, *Astrophys. J.* **224**, L113
Becker, R.H., Rothschild, R.E., Boldt, E.A., Holt, S.S., Pravdo, S.H., Serlemitsos, P.J., Swank, J.H.: 1978b, *Astrophys. J.* **221**, 912
Bethe, H.A., Salpeter, E.E.: 1957, Quantum Mechanics of One- and Two-Electron Systems, Academic Press, New York
Boldt, E.A.: 1977, *Ann. N.Y. Acad. Sci.* **302**, 329
Buff, J., McCray, R.: 1974, *Astrophys. J.* **189**, 147
Burbidge, G.R., Gould, R.J.: 1963, *Astrophys. J.* **138**, 945
Burgess, A.: 1964, *Mem. Roy. Astron. Soc.* **69**, 1
Chandrasekhar, S.: 1960, Radiative Transfer, Dover Publ., N.Y.
Felten, J.E., Rees, M.J., Adams, T.F.: 1972, *Astron. Astrophys.* **21**, 139
Ghosh, P., Lamb, F.K.: 1978, *Astrophys. J.* **223**, L83
Hatchett, S., Weaver, R.: 1977, *Astrophys. J.* **215**, 285
Ivanov, V.V.: 1969, *Radiative Transfer and Spectra of Celestial Bodies*, Nauka, Moscow
Jacobs, A.: 1972, *J. Quant. Spectroscop. Radiat. Transfer* **12**, 243
Kestenbaum, H.L., Long, K.S., Novick, R., Weisskopf, M.C., Wolff, R.S.: 1977, *Astrophys. J.* **216**, L19
Kestenbaum, H.L., Ku, W.H.-M., Long, K.S., Silver, E.H., Novick, R.: 1978, *Astrophys. J.* **226**, 282
Lamb, F.K., Pethick, C.J., Pines, D.: 1973, *Astrophys. J.* **184**, 271

Lotz, W.: 1967, *Astrophys. J. Suppl.* **14**, 207
McCray, R., Lamb, F.K.: 1976, *Astrophys. J.* **204**, L115
Mészàros, P.: 1974, *Astron. Astrophys.* **35**, 171
Milgrom, M.: 1976, *Astron. Astrophys.* **51**, 215
Pravdo, S.H.: 1978 (preprint)
Pravdo, S.H., Becker, R.H., Boldt, E.A., Holt, S.S., Serlemitsos, P.J., Swank, J.H.: 1977, *Astrophys. J.* **215**, L61
Pravdo, S.H., Bussard, R.W., Becker, R.H., Boldt, E.A., Holt, S.S., Serlemitsos, P.J., Swank, J.H.: 1978, *Astrophys. J.* **225**, L53
Ross, R.R., Weaver, R., McCray, R.: 1978, *Astrophys. J.* **219**, 292
Sanford, P.W., Mason, K.O., Ives, J.: 1975, *Monthly Notices Roy. Astron. Soc.* **173**, 9P
Scharlemann, E.: 1978, *Astrophys. J.* **219**, 617
Serlemitsos, P.J., Boldt, E.A., Holt, S.S., Rothschild, R.E., Saba, J.L.R.: 1975, *Astrophys. J.* **201**, L9
Shulman, S., Friedman, H., Fritz, G., Henry, R.C., Yentis, D.J.: 1975, *Astrophys. J.* **199**, L101
Sunyaev, R.A.: 1976a, *Pisma Astron. Zh. (Letters to Soviet Astronomy)* **2**, 287
Sunyaev, R.A.: 1976b, *Pisma Astron. Zh. (Letters to Soviet Astronomy)* **2**, 334
Swank, J.H.: 1977 (private communication)
Tarter, C.B., Tucker, W.H., Salpeter, E.E.: 1969, *Astrophys. J.* **156**, 943
Vainshtein, L.A., Safronova, U.I.: 1977, in *Spectroscopic Constants of Atoms*, Part 1, Acad. Sci. USSR, Moscow